

JPL D-11507, Rev. E  
December 13, 1999

Multi-angle Imaging SpectroRadiometer (MISR)

# **Level 1 Radiance Scaling and Conditioning Algorithm Theoretical Basis**

Approvals:

David J. Diner  
MISR Principal Investigator

Thomas R. Livermore  
MISR Project Manager

Graham W. Bothwell  
MISR Science Data System Manager

The MISR web site should be consulted to determine the latest released version of this document (<http://www-misr.jpl.nasa.gov>). Approval signatures are on file with the MISR Project.



**Jet Propulsion Laboratory**  
California Institute of Technology

## TABLE OF CONTENTS

1. INTRODUCTION .....	1
1.1 PURPOSE.....	1
1.2 SCOPE .....	2
1.3 MISR DOCUMENTS.....	3
1.4 REVISIONS .....	3
2. EXPERIMENT OVERVIEW.....	5
2.1 OBJECTIVES OF MISR RADIANCE SCALING AND CONDITIONING .....	5
2.2 INSTRUMENT FEATURES .....	6
2.2.1 On-Board Calibrator .....	7
2.2.1.1 Diffuse panels .....	7
2.2.1.2 Calibration photodiodes .....	7
2.2.1.3 Goniometer .....	7
2.3 CALIBRATION APPROACH.....	8
2.3.1 Spectral calibration (pre-flight only) .....	8
2.3.2 Radiometric calibration (pre-flight and in-flight) .....	10
3. ALGORITHM DESCRIPTION .....	11
3.1 NOMENCLATURE .....	11
3.2 PROCESSING OUTLINE .....	12
3.3 ALGORITHM INPUT .....	13
3.3.1 Level 0 Instrument Digital Numbers .....	13
3.3.2 Level 1A Cal-CCD data and IDQI parameters .....	14
3.3.3 Ancillary Radiometric Product data.....	14
3.3.3.1 Out-of-range threshold parameters .....	14
3.3.3.2 Detector Data Quality Indicators .....	15
3.3.3.3 Radiometric calibration coefficients.....	15
3.3.3.4 PSF deconvolution functions .....	16
3.4 THEORETICAL DESCRIPTION .....	16
3.4.1 Reverse square-root encoding .....	16
3.4.1.1 Processing objectives .....	16
3.4.1.2 Mathematical description of the algorithm.....	17
3.4.2 Radiance scaling .....	17
3.4.2.1 Processing objectives .....	17
3.4.2.2 Mathematical description of the algorithm.....	17
3.4.3 Perform scene-dependent quality assessment .....	18
3.4.3.1 Processing objectives .....	18
3.4.3.2 Mathematical description of the algorithm: Part 1, L1A Cal-packets .....	19
3.4.3.3 Mathematical description: Part 2, L1A Science-packets .....	21
3.4.4 Establish combined data quality indicators .....	25
3.4.4.1 Processing objectives .....	25

3.4.4.2 Mathematical description of the algorithm. . . . .	25
3.4.5 Radiance conditioning: Image restoration . . . . .	26
3.4.5.1 Processing objectives . . . . .	26
3.4.5.2 Mathematical description of the algorithm. . . . .	27
3.4.6 Separate Global and Local Mode data. . . . .	29
3.4.6.1 Processing objectives . . . . .	29
3.4.6.2 Mathematical description of the algorithm. . . . .	29
3.4.7 Scale output . . . . .	29
3.4.7.1 Processing objectives . . . . .	29
3.4.7.2 Mathematical description of the algorithm. . . . .	29
3.5 PRACTICAL CONSIDERATIONS. . . . .	30
3.5.1 Numerical computation considerations. . . . .	30
3.5.2 Programming and procedural considerations. . . . .	30
3.5.3 Configuration of software . . . . .	30
3.5.4 Quality assessment and diagnostics. . . . .	31
3.5.5 Exception handling . . . . .	31
3.14 ALGORITHM VALIDATION. . . . .	31
3.15 ALGORITHM DEVELOPMENT SCHEDULE . . . . .	32
4. ASSUMPTIONS AND LIMITATIONS . . . . .	33
4.1 ASSUMPTIONS. . . . .	33
4.2 LIMITATIONS. . . . .	33
5. REFERENCES . . . . .	34

## ACRONYMS

### A

ARP Ancillary Radiometric Product  
ATB Algorithm Theoretical Basis

### C

CCD Charge-Coupled Device

### D

DAAC Distributed Active Archive Center  
DDQI Detector Data Quality Indicator  
DN digital number

### E

EOS Earth Observing System

### F

FWHM Full-Width at Half Maximum

### G

GRP Georectified Radiance Product

### H

HQE high quantum efficiency

### I

IDN Instrument Digital Numbers  
IDQI Image Data Quality Indicator  
IFRCC In-flight Radiometric Calibration and Characterization  
IR infrared

### L

LSB Least Significant Bit

### M

MISR Multi-angle Imaging SpectroRadiometer  
MKS meter, kilogram, second  
MODIS Moderate Resolution Imaging Spectroradiometer  
MSB Most Significant Bit

### O

OBC On-Board Calibrator

### P

PIN p/intrinsic/n doped layers  
PSF point spread function  
PTFE polytetrafluoroethylene

**Q**

QE            quantum efficiency

**R**

RDQI        Radiometric Data Quality Indicator

**S**

SCF           Science Computing Facility

SDQI        Scene-dependent Data Quality Indicator

SI            Système International

SNR          signal-to-noise ratio

# 1. INTRODUCTION

## 1.1 PURPOSE

This Algorithm Theoretical Basis (ATB) document describes the algorithms used to produce the Multi-angle Imaging SpectroRadiometer (MISR) Level 1B1 Radiometric Product, and certain parameters of the Level 1A Reformatted Annotated Product. Conversion of 12-bit instrument digital numbers (IDN) to 14-bit numbers (referred to as DN) is a primary objective of Level 1A processing. DN conversion to spectral radiances (known as radiance scaling), radiometric data quality assessment, and radiance conditioning to compensate for certain performance characteristics of the MISR instrument are the primary objectives of Level 1B1 processing. Both products are generated at the Distributed Active Archive Center (DAAC). The processing is done routinely on all transmitted MISR charge-coupled device (CCD) imaging data, including data acquired in both Science and Calibration modes, and is used to construct a data set from which all other MISR standard data products follow. The Level 1A product parameters discussed in this document are summarized in Table 1.1. A more complete listing of the Level 1A product contents is provided in [DPS] (document abbreviations defined in §1.3). The Level 1B1 product parameters are summarized in Table 1.2. The radiometric data have the same spatial sampling as in the Level 1A product.

**Table 1.1. Level 1A Reformatted Annotated Product (partial listing)**

<b>Parameter name</b>	<b>Units</b>	<b>Horizontal Sampling (Coverage)</b>	<b>Comments</b>
CCD Science Data (DN)	none	250 m nadir, 275 m off-nadir, or averages per the camera configuration (Global)	<ul style="list-style-type: none"><li>• Square-root encoding reversed</li><li>• No geometric resampling</li><li>• 9 cameras, 4 bands</li></ul>
Science Data Image Data Quality Indicator	none	Associated with each DN	<ul style="list-style-type: none"><li>• Values: 0 (within specification), 1 (reduced accuracy), 2 (not usable for science), and 3 (unusable)</li><li>• Stored as the two least significant bits in the radiance integer fields</li></ul>
CCD Calibration Data (DN)	none	250 m nadir, 275 m off-nadir, or averages per the camera configuration	<ul style="list-style-type: none"><li>• Square-root encoding reversed</li><li>• No geometric resampling</li><li>• 9 cameras, 4 bands</li></ul>
Calibration Data Image Data Quality Indicator	none	Associated with each DN	<ul style="list-style-type: none"><li>• Values: 0 (no known anomalies), 1 (overclock out-of-range), 2 (saturated pixel), and 3 (data transmission error)</li><li>• Stored as the two least significant bits in the radiance integer fields</li></ul>

**Table 1.2. Level 1B1 Radiometric Product**

<b>Parameter name</b>	<b>Units</b>	<b>Horizontal Sampling (Coverage)</b>	<b>Comments</b>
Radiance (Global Mode and Local Mode)	$\text{W m}^{-2}$ $\mu\text{m}^{-1} \text{sr}^{-1}$	250 m nadir, 275 m off-nadir, or averages per the camera configuration (Global and Regional)	<ul style="list-style-type: none"> <li>• Radiometrically-scaled data in range 0-16376</li> <li>• Values 16377-16383 reserved for L1B2 flag values</li> <li>• No geometric resampling</li> <li>• 9 cameras, 4 bands</li> <li>• Radiometric uncertainties reported in the Ancillary Radiometric Product</li> </ul>
Flag Data	none	Replaces radiance data where there is a retrieval error	<ul style="list-style-type: none"> <li>• Values: 16377 through 16383</li> </ul>
Image Data Quality Indicator	none	Associated with each DN	<ul style="list-style-type: none"> <li>• Values: 0 (within specification), 1 (reduced accuracy), 2 (not usable for science), and 3 (unusable)</li> <li>• Stored as the two least significant bits in the radiance integer fields.</li> </ul>

The algorithms used to produce the Level 1A and 1B1 products require knowledge of data quality associated with each of the CCD detector elements, the camera radiometric calibration coefficients, and other parameters associated with instrument spectral calibration. These inputs are summarized and distributed to the scientific community through the Level 1 Ancillary Radiometric Product (ARP). The ARP is generated at the MISR Science Computing Facility and delivered to the DAAC. It consists of four structures: a Preflight Characterization file, a Preflight Calibration file, an In-flight Calibration file, and a Configuration Parameters file. The first contains parameters that are provided to the science user for their reference. These are not utilized in any DAAC processing algorithm. The calibration and configuration parameters are needed DAAC inputs; however, only the in-flight calibration parameters are recomputed and delivered at routine intervals (nominally, monthly). Production of the ARP is not part of the routine DAAC processing of MISR data; rather, it is the responsibility of the MISR In-flight Radiometric Calibration and Characterization (IFRCC) team. The contents of the ARP and the algorithms used to generate it are described in [IFRCC ATB].

## 1.2 SCOPE

This document identifies sources of input data, provides a background to the algorithm selection, and gives a mathematical description of the processes to be used for radiance scaling, radiance conditioning, and data quality assessment. It also describes practical considerations which must be factored into the algorithm development. Chapter 1 defines the Level 1A and Level 1B1 data product contents that are covered by this ATB, and lists MISR project documents which specify the calibration requirements, or are otherwise relevant to the calibration activities. Chapter 2 gives an overview of the instrument, calibration, and calibration requirements. Chapter 3 gives the theoretical basis of the relevant portions of Level 1A and Level 1B1 processing. Chapter 4 lists assumptions and limitations. Chapter 5 provides a list of open literature references.

### 1.3 MISR DOCUMENTS

Throughout this document a notation of the form [shorthand] will be used to reference project documents. These abbreviations are defined in this section. Open literature references are pointed to by means of superscript numbers in the text. These numbers refer to the publications listed in Chapter 5.

[Exp]	Experiment Overview, JPL D-13407.
[ISR]	Instrument Science Requirements, JPL D-9090, Rev. B.
[FDR]	Instrument Functional and Design Requirements, JPL D-9988.
[CalMgmt]	Calibration Management Plan, JPL D-7463.
[PreCal]	Preflight Calibration Plan, JPL D-11392.
[IFRCC Plan]	In-flight Radiometric Calibration and Characterization Plan, JPL D-13315.
[IFRCC ATB]	Level 1 In-flight Radiometric Calibration and Characterization Algorithm Theoretical Basis, JPL D-13398.
[GeoCal Plan]	In-flight Geometric Calibration Plan, JPL D-13228.
[GRP ATB]	Level 1 Georectification and Registration Algorithm Theoretical Basis, JPL D-11532, Rev. B.
[DSSR]	Data System Science Requirements, JPL D-11398.
[DPS]	Data Product Specifications Document, JPL D-12941, Rev. C.
[ADP]	Algorithm Development Plan, JPL D-11220.
[DPSize]	Science Data Processing Sizing Estimates, JPL D-12569.

### 1.4 REVISIONS

This is Revision E. Changes from Revision D are:

- The Data Product Description document is replaced with the Data Product Specifications document.
- In §3.4.5 the algorithm for image restoration is changed. PSF deconvolution functions have been added to the ARP, and parameters relating to PSF convergence have been deleted.

Changes from Revision C to D were:

- In §3.3.2 the algorithm for producing the L1A SDQI parameters are specified.
- In §3.4.3.3.1 the SDQI values was changed from 3 to 2, for those pixels in the vicinity of a saturated pixel.

Changes from Revision B to C were :

- The case where radiance is to be retrieved, when  $G_2=0$ , is defined (see Eqn. (3.3)).
- A quality flag is defined for the case where the PSF deconvolution does not converge (see §3.4.5.2).
- In the PSF deconvolution algorithm, §3.4.5.2, the expected pixel-to-pixel uncertainty now makes use of a systematic uncertainty,  $\epsilon_{\text{pix\_sys}}$ .
- The data quality flag definitions have been revised.
- The use of flag-values, in the event of a unusable radiance retrieval, and packing of the Image Data Quality Indicator values into the two least-significant bits is specified.

Changes from the original revision to Revision B were that the previous two releases went by a different title:

- MISR Level 1B1 Radiometric Product Algorithm Theoretical Basis, JPL D-11507, Rev. A, 01 Nov. 1994.
- MISR Level 1B1 Radiometric Product Algorithm Theoretical Basis, JPL D-11507, 23 Feb. 1994.

Revisions to this document will be approved by the MISR Principal Investigator and the MISR Instrument Scientist.

## 2. EXPERIMENT OVERVIEW

### 2.1 OBJECTIVES OF MISR RADIANCE SCALING AND CONDITIONING

The only directly measured observables acquired by MISR are camera incident radiances. All geophysical parameters are derived from these data (see [Exp] and [DPS]). Yet, the DN transmitted by MISR only provide an accurate measure of these radiances once a series of processing steps, called radiance scaling and conditioning, have been performed. During these steps the DN values are converted to spectral radiances, and reported in MKS (meter, kilogram, second) units referred to as SI (Système International)<sup>1</sup>. Radiances are weighted over the total band response. To produce these radiances, use is made of an inverse operation, radiometric calibration, where the response of the system to a known radiance field is determined. The radiometric calibration represents our best estimate of the response under controlled illumination conditions, as determined through many different activities conducted both preflight and in-flight.

MISR data are intended to support a variety of users, each with different research interests and radiometric accuracy requirements. In general, uncertainties in geophysical parameters derived from remote sensing measurements arise from measurement errors, limitations imposed by the finite spatial, spectral, angular, and temporal resolution and coverage of the data, and factors inherent in the algorithms used to process the data. The goal in MISR calibration is to keep errors due to instrument performance below the level of imperfection associated with the data reduction process, thus allowing the possibility of later improvements in the algorithms.

In terms of absolute radiometry, MISR performance is driven by the desire to:

- (1) Determine changes in the solar radiation budget, and thus provide data for global climate studies;
- (2) Produce a data set of value to long-term monitoring programs and allow intercomparisons of data on time scales exceeding that of an individual satellite;
- (3) Provide Earth Observing System (EOS) synergism, and allow data exchanges between EOS-platform instruments.

In order to keep instrumental errors from being the limiting source of uncertainty associated with estimation of radiances using MISR data, we adopt a performance requirement of 3% absolute uncertainty ( $1\sigma$ / full scale). This will be provided through the use of detector-based calibration standards (these detectors and the diffuse panels constitute the on-board calibration hardware), and vicarious calibrations. Verifications include cross-comparisons using targets viewed in common with the Moderate Resolution Imaging Spectroradiometer (MODIS).

Not all of the MISR measurement objectives are dependent upon high absolute accuracies. For example, the determination of the shape of angular reflectance signatures of surfaces and clouds are dependent on the relative camera-to-camera and band-to-band radiometric accuracy. The requirements for these calibrations are such that sufficient accuracy is achieved for studies making use of directional reflectances.

It is noted that MISR does not provide a Level 1B1 reflectance product scaled to the exo-atmospheric solar irradiance. As MISR does not view the Sun directly, such a data set could only be obtained by employing a solar model, and would be of no greater accuracy than the radiance product.

## 2.2 INSTRUMENT FEATURES

MISR is part of an Earth Observing System (EOS) payload to be launched in 1998. The instrument consists of nine pushbroom cameras. It is capable of global coverage every nine days, and flies in a 705-km descending polar orbit. The cameras are arranged with one camera pointing toward the nadir (designated An), one bank of four cameras pointing in the forward direction (designated Af, Bf, Cf, and Df in order of increasing off-nadir angle), and one bank of four cameras pointing in the aftward direction (using the same convention but designated Aa, Ba, Ca, and Da). Images are acquired with nominal view angles, relative to the surface reference ellipsoid, of 0°, 26.1°, 45.6°, 60.0°, and 70.5° for An, Af/Aa, Bf/Ba, Cf/Ca, and Df/Da, respectively. Each camera uses four Charge-Coupled Device (CCD) line arrays in a single focal plane. The camera outputs consist of 1504 photoactive pixels, plus 8 light-shielded pixels (not utilized), each 21  $\mu\text{m}$  (cross-track) x 18  $\mu\text{m}$  (along-track) in size. Additionally there are 8 “overclock” samples of the contents of the CCD serial registers. Each line array is filtered to provide one of four MISR spectral bands. The spectral band shapes are nominally gaussian with bandcenters at 446, 558, 672, and 866 nm (as determined by an in-band, solar-weighted moments analysis). The instrument contains 36 channels, corresponding to 4 bands in each of 9 cameras.

MISR will acquire images in each of its channels with spatial sampling ranging from 275 m (250 m cross-track in the nadir) to 1.1 km (1.0 km cross-track in the nadir), depending on the on-board pixel averaging mode used prior to transmission of the data. The instrument is capable of buffering the data to provide 4x4, 2x2, or 1x4 detector cross-track x along-track pixel averages, in addition to the 1x1 mode in which pixels are sent with no averaging. The averaging capability is individually selectable within each of the 36 channels. A particular averaging selection among the 36 channels is referred to as the camera configuration.

There are several observational modes of the MISR instrument. Global Mode is the default mode, and refers to continuous operation with no limitation on swath length. Global coverage in a particular spectral band of one camera is provided by operating the corresponding signal chain continuously in a selected resolution mode. Any choice of averaging modes among the nine cameras that is consistent with the instrument power and data rate allocation is suitable for Global Mode. Additionally, Local Mode provides high resolution images in all 4 bands of all 9 cameras for selected Earth targets. This is accomplished by inhibiting pixel averaging in all bands of each of the cameras in sequence, one at a time, beginning with the first camera to acquire the target and ending with the last camera to view the target. The instrument geometry limits the along-track length of Local Mode targets to about 300 km. Finally, in Calibration Mode the on-board calibration hardware is utilized, and calibration data are acquired for the cameras. There are four Calibration Modes, as described in [IFRCC Plan]. The Cal-North and Cal-South Modes provide an on-orbit radiometric calibration of the cameras. Data will be obtained for each spatial sampling mode by cycling each channel through the various modes during the calibration period. This will occur on a monthly basis during routine mission operations, although early in the mission it will

be used more frequently. Cal-Dark determines the dark-current response of the cameras and photodiodes; Cal-Diode images the Earth, in order to confirm photodiode response stability.

### **2.2.1 On-Board Calibrator**

#### **2.2.1.1 Diffuse panels**

A key component of the MISR On-Board Calibrator (OBC) is a pair of deployable, diffuse panels. These have a high, near-lambertian reflectance. While not in use the panels are stowed and protected. At approximately monthly intervals the panels are deployed for calibration. Over the North Pole, a panel will swing aftward to diffusely reflect sunlight into the fields-of-view of the aftward-looking and nadir cameras. Over the South Pole, the other panel will swing forward for calibration of the forward-looking and nadir cameras. The nadir camera will provide a link between the two sets of observations. Cumulative space exposure time (deploy time) for each panel is expected to be less than 100 hours over the mission life.

After a materials search, Spectralon™ (a product of Labsphere, New Hampshire) has been selected for the MISR in-orbit calibration targets. Spectralon is composed of pure polytetrafluoroethylene (PTFE, or Teflon) polymer resin which is compressed and sintered. MISR has provided for the flight qualification of this material.

#### **2.2.1.2 Calibration photodiodes**

The diffuse calibration targets will be monitored by three types of diodes: radiation-resistant PIN photodiodes and two types of high quantum efficiency (HQE) diodes. (Note "PIN" is a description of the diode architecture where  $p$ , intrinsic, and  $n$  doped layers are stacked.) The radiation-resistant photodiodes will be fabricated four to a package, each diode filtered to a different MISR spectral band. The fields-of-view are approximately  $8^\circ$ , sufficient to allow the required signal-to-noise ratio (SNR) of 500 to be achieved. Five such packages will be used. Two will view in the nadir direction, one in each of the Df and Da camera directions, and one package will be mechanized on a goniometric arm to monitor the angular reflectance properties of the panels.

The HQE's are in a "trap" configuration. Three silicon photodiodes are arranged in a package so that light reflected from one diode is absorbed by another diode. The output of each diode is summed in parallel, resulting in near 100% quantum efficiency. A single spectral filter per package is used, and four such packages provide coverage at the four MISR wavelengths. One diode type, optimized for high quantum efficiency (QE) in the blue, is used within those packages which cover three of the four MISR bands (the blue, green, and red bands). A design optimized for high QE in the red is used in the package using the near-IR filter. Stability through mission life, as well as spectral QE data were considered in this selection.

#### **2.2.1.3 Goniometer**

The goniometer is a device that characterizes the relative diffuse panel radiance function with angle. It does so in a plane parallel to the spacecraft flight direction. A PIN package mounted

to the goniometer arm swings through  $\pm 60^\circ$  to allow panel characterization appropriate to the along-track camera angles.

## 2.3 CALIBRATION APPROACH

MISR will be calibrated pre-flight in terms of its spectral and radiometric response (see [CalMgmt], [PreCal]), and in-flight in terms of its radiometric response (see [IFRCC Plan]). In addition, geometric characterizations of boresight and boresight changes with temperature, and camera pointing repeatability with temperature will be obtained, and a calibrated geometric camera model will be generated in-flight using ground control points (see [PreCal], [GeoCal Plan]). Performance reports will be delivered to the DAAC for archival. Raw camera and ancillary data and processing codes will be archived at the SCF.

A brief description of the spectral and radiometric coefficients is given below. The data sets and processing algorithms used to generate these and other ARP products is given in [IFRCC ATB].

### 2.3.1 Spectral calibration (pre-flight only)

The pre-flight spectral calibration of the MISR cameras has been used to establish the pixel-by-pixel spectral response within each of the instrument's 36 channels. These measured spectral response curves are denoted  $R_{\lambda,p}$  and depicted schematically in Figure 2.1. The "in-band" region is defined to be the spectral range over which the response exceeds 1% of the peak response. The measured data include the effects of the optics, filter, and detector response with wavelength. The MISR cameras are found to have a non-negligible response (system transmittance in the range  $10^{-4}$  to  $10^{-3}$ ) outside of the in-band region. Thus, the radiances reported at Level 1B1 contain contributions from the out-of-band region.

Spectral calibration is performed at the camera level (prior to assembly onto the instrument optical bench) under thermal vacuum conditions. The spectral response is established by using a monochromator and laboratory detector-based standards (trapped HQE silicon photodiodes). The monochromator provides an illumination source of varying spectral output, while the laboratory standards measure this variation with wavelength. These latter data are used to normalize the camera output, such that the camera response to an effective source of constant radiance, but varying color, can be determined. It is noted that the spectral response so determined is a function of the instrument properties alone, independent of an assumption of the scene spectral properties. Measurements are acquired at a set of discrete locations within the fields of view of each camera. Response curves for pixels not directly measured during this calibration are obtained by interpolation. This characterization is processed to provide data which appear in the Ancillary Radiometric Product (ARP).

Because there are slight (a few nm) shifts in band center and bandwidth across the fields of view of each camera, and from camera to camera, as well as small variations in the out-of-band response, standardized spectral response profiles are derived from the  $R_\lambda$  curves and stored in the ARP. The standardized spectral response profiles are derived by averaging all measured  $R_\lambda$  curves within a given spectral band. This generates a set of four standardized response curves, one for

each band, denoted  $S_\lambda$ . This function is depicted schematically in Figure 2.1. The in-band portion of each standardized response curves is denoted  $S_\lambda^{\text{in-band}}$ . Based upon these spectral response curves, the ARP includes information summarized in Tables 2.1 and 2.2 (see [IFRCC ATB]).

**Table 2.1. Spectral profile functions contained in the ARP**

Function name	Description
$R_\lambda$	Measured pixel-by-pixel spectral response curves
$S_\lambda$	Standardized band-by-band spectral response curves
$S_\lambda^{\text{in-band}}$	In-band portion of $S_\lambda$

**Table 2.2. Spectral summary parameters contained in the ARP**

Parameter name	Description
$\lambda_l^{\text{std}}$ and $\lambda_u^{\text{std}}$	Wavelengths delimiting the lower and upper bounds of the standardized in-band region
$\lambda_m^{\text{meas}}$ and $\Delta\lambda_m^{\text{meas}}$	Pixel-by-pixel central wavelengths and equivalent square bandwidths, derived from a moments analysis of $R_\lambda$
$\lambda_m^{\text{std}}$ and $\Delta\lambda_m^{\text{std}}$	Band-by-band central wavelengths and equivalent square bandwidths, derived from a moments analysis of $S_\lambda$
$\lambda_g^{\text{meas, in-band}}$ and $\Delta\lambda_g^{\text{meas, in-band}}$	Pixel-by-pixel central wavelengths and full-width at half maximum (FWHM) bandwidths, derived from a gaussian best-fit analysis of the in-band portion of $R_\lambda$
$\lambda_g^{\text{std, in-band}}$ and $\Delta\lambda_g^{\text{std, in-band}}$	Band-by-band central wavelengths and FWHM bandwidths, derived from a gaussian best-fit analysis of $S_\lambda^{\text{in-band}}$
$\lambda_{m, \text{solar}}^{\text{std}}$ and $\Delta\lambda_{m, \text{solar}}^{\text{std}}$	Band-by-band central wavelengths and equivalent square bandwidths, derived from a total-band moments analysis of $E_{0\lambda} \cdot S_\lambda$ , i.e., including a weighting by spectral exo-atmospheric solar irradiance
$\lambda_{m, \text{solar}}^{\text{std, in-band}}$ and $\Delta\lambda_{m, \text{solar}}^{\text{std, in-band}}$	Band-by-band central wavelengths and equivalent square bandwidths, derived from an in-band moments analysis of $E_{0\lambda} \cdot S_\lambda^{\text{in-band}}$ , i.e., including a weighting by spectral exo-atmospheric solar irradiance

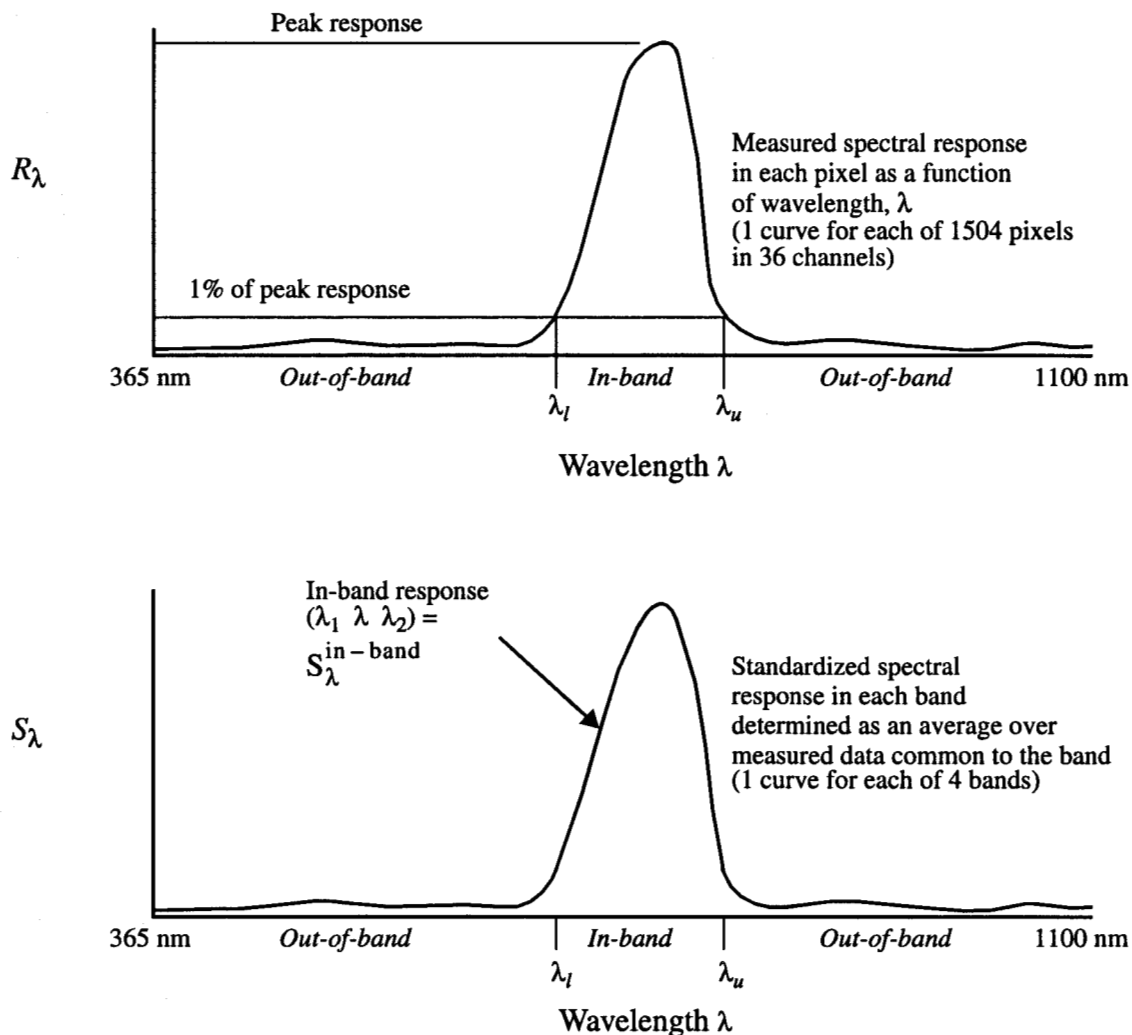


**Figure 2.1. Spectral response curve definitions**

### 2.3.2 Radiometric calibration (pre-flight and in-flight)

During radiometric calibration the relationship between an incident radiance field and camera digital output is established (i.e., the radiometric transfer curve). This is done using an “ideal” target which emits or reflects unpolarized light, is uniform in space and angle, and lacking in spectral features such as absorption lines. JPL’s 1.65-m diameter integrating sphere was used as such a target during preflight calibration. The sphere-emitted radiance was determined by using photodiode laboratory standards (i.e., trapped HQE silicon photodiodes). Data acquired during the EOS mission using the MISR instrument OBC, image data, and field campaigns will provide the in-flight calibration. These activities are undertaken to determine the calibration equation coefficients. The methodology is described in [IFRCC Plan], and the theoretical basis of the algorithms to be used to determine the calibration coefficients is presented in [IFRCC ATB]. Determination of the instrument calibration coefficients involves a regression of data numbers for each sample of data acquired by the cameras against radiances which are normalized to the standardized response profiles. Thus, Level 1B1 generates radiances based on standardized spectral response profiles.

### 3. ALGORITHM DESCRIPTION

#### 3.1 NOMENCLATURE

As discussed in Chapter 2, the process termed radiometric calibration is used to determine the calibration coefficients which relate the sensor output DN to the incoming radiance. In the reverse process, radiance scaling, DN data from a camera are transformed onto a radiometric scale. This is done by making use of these same calibration coefficients. For a scene which is similar to the flat-field calibration target (uniform, spectrally flat, unpolarized) this radiance scaling is, in most cases, sufficient to compute a measure of the incident radiance. This relationship between sensor calibration and radiance scaling is shown pictorially in Figure 3.1.

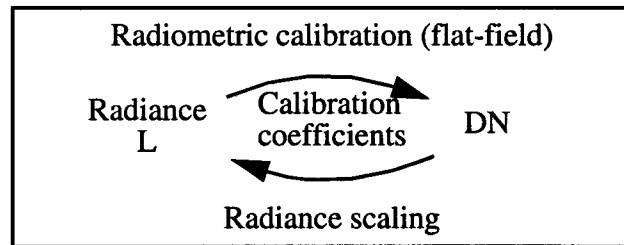


**Figure 3.1. Relationship between radiometric calibration and radiance scaling**

During scene response characterization of the sensor's point spread function (PSF), pixel-to-pixel response non-uniformity, spectral out-of-band response, and noise properties are determined. These effects can result in a radiometric error in the computed radiance, if sufficient in magnitude. This error is a function of scene type (divergence from the featureless calibration target). The processing termed radiance conditioning is utilized to convert the imperfect image into a better representation of the original scene. Correction for the PSF response of the cameras is the only processing step currently envisioned necessary as part of radiance conditioning. The relationship between scene response characterization and radiance conditioning is shown pictorially in Figure 3.2.

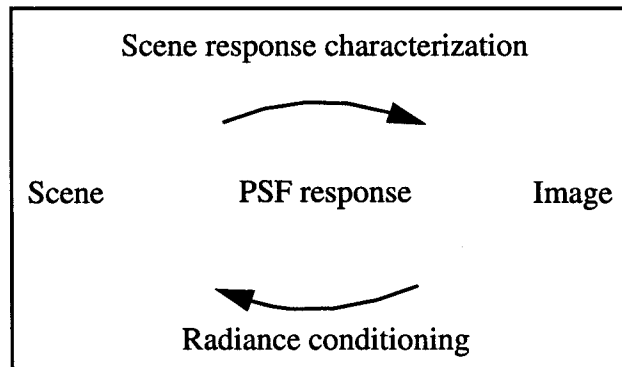


**Figure 3.2. Relationship between scene response characterization and radiance conditioning**

## 3.2 PROCESSING OUTLINE

The processing flow for the portion of generation of the Level 1A Reformatted Annotated Product dealing with radiometric image data and for the Level 1B1 Radiometric Product is shown in Figure 3.3, along with a symbol convention. They are shown as part of a combined flow because it is currently envisioned that the Level 1A product will be archived, whereas the Level 1B1 product will be held temporarily only until the completion of Level 1B2 processing. Users interested in the Level 1B1 product will be able to obtain it "on-demand".

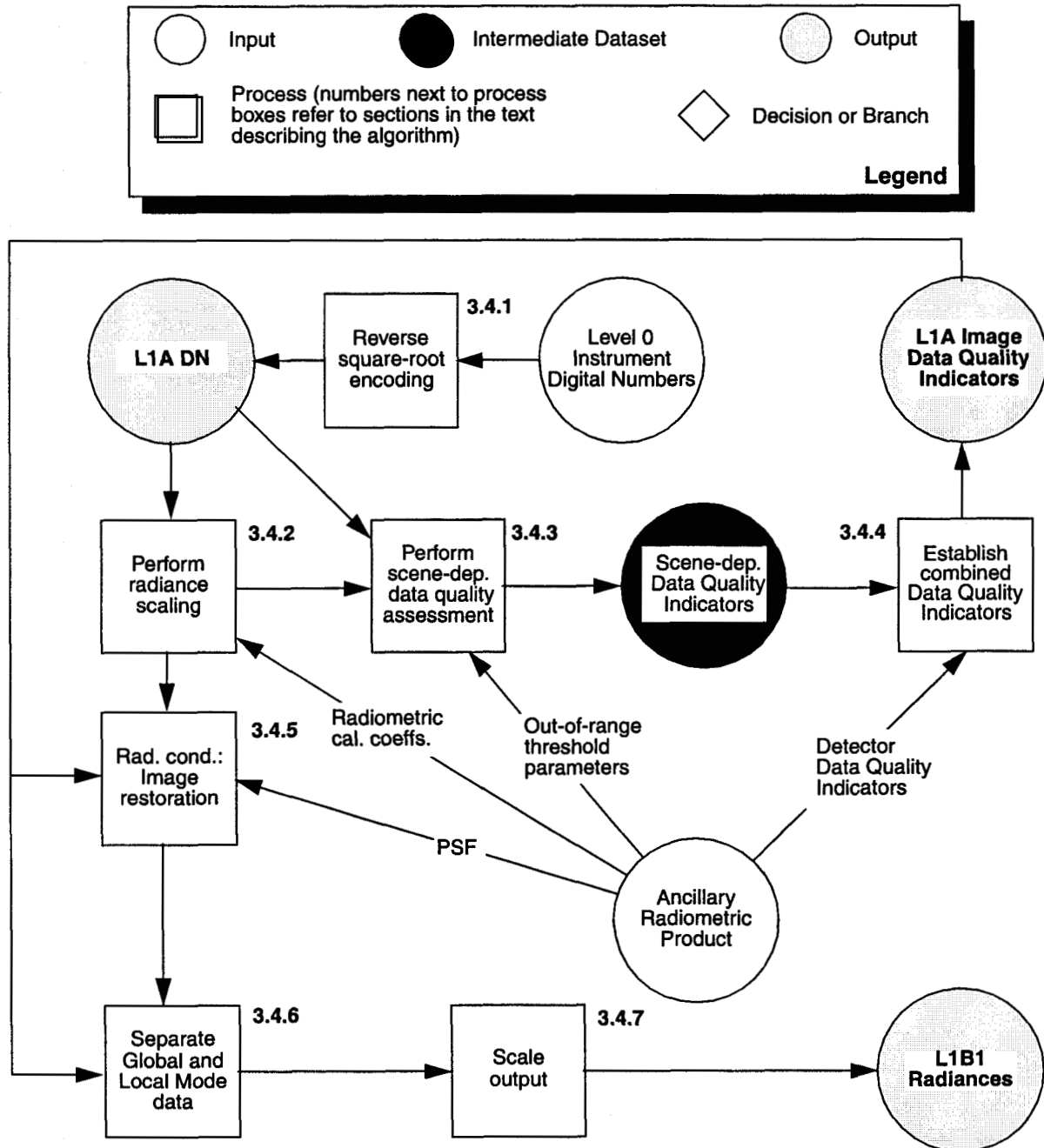


**Figure 3.3. Generation of the science data in the Level 1A and Level 1B1 products**

The scene-dependent data quality assessment parameters report on loss of radiometric integrity due to saturation, or other anomalous conditions. Radiance scaling uses coefficients, generated at the MISR Science Computing Facility (SCF) and reported in the Ancillary Radiometric Product, to convert digital numbers to radiances. These coefficients represent our latest understanding of each pixel's response function, and are derived as described in [IFRCC ATB] and [IFRCC Plan]. Radiance conditioning consists of point-spread-function (PSF) deconvolution to provide an image restoration step to compensate for low-level halos in the camera impulse response. The rationale behind the radiance conditioning process arises from an understanding of the actual camera performance characteristics, obtained during pre-flight testing. The output product consists of radiance values corresponding to each Level 1A input value. Additionally, data integrity metrics are reported with the Level 1A product.

### 3.3 ALGORITHM INPUT

Required inputs for the process described in this ATB are summarized in Table 3.1. No non-MISR data are required.

**Table 3.1. Processing inputs**

Input data	Source of data	Reference
Instrument Digital Numbers (IDN)	Level 0 or Level 1A Raw Data	[DPS]
Out-of-range threshold parameters	Ancillary Radiometric Product	[IFRCC ATB], [IFRCC Plan]
Detector Data Quality Indicators	Ancillary Radiometric Product	[IFRCC ATB], [IFRCC Plan]
Radiometric calibration coefficients	Ancillary Radiometric Product	[IFRCC ATB], [IFRCC Plan]
PSF deconvolution functions	Ancillary Radiometric Product	[IFRCC ATB], [IFRCC Plan]

#### 3.3.1 Level 0 Instrument Digital Numbers

Square-root encoding is performed in-flight in order to compress MISR camera data and prepare for transmission. Thus, the 14-bit data which are produced by an individual camera are square-root encoded, through use of a table look-up process, and reduced to 12-bit Instrument Digital Numbers (IDN).

The MISR arrays pass 1520 IDN values per channel, in the unaveraged (1x1) and 1x4 camera configurations. The first 1504 values are from the active CCD area, and contain scene brightness information. The next eight pixels are from light-shielded pixels, which were intended to be a measure of the video offset DN. In practice, pinholes in the aluminum overcoat produce light leaks, and these shielded pixels are therefore ignored. The next eight pixel values are called overclock pixels. These pixels are samples of the serial register, after all physical pixels have

clocked out. For this reason, the overclock pixels are used to generate a measure of the video offset for each channel. This video offset is dynamic; a unique value is determined for each line of CCD data. This value, called  $D_{overclock}$ , is used in the radiance scaling algorithm for all samples in the line.

In 2x2 averaging mode, there are 752 science data samples, 4 shielded pixel values, and 4 overclock sample values. In 4x4 averaging mode, there are 376 science data samples, 2 shielded pixel values, and 2 overclock sample values.

### 3.3.2 Level 1A Cal-CCD data and IDQI parameters

The Level 1A CCD data, acquired as part of an on-orbit calibration experiment, are called the L1A Cal-CCD data. These data are distinct from the science CCD data, and are identified with an APID code (packet identification number). These L1A data include both radiance data and an Image Data Quality Indicator (IDQI) parameters. The IDQI values are packed as the least significant 2 bits of the DN data. For the Cal product, IDQI=3 generally indicates a data transmission or packet out-of-sync problem. IDQI=1 or 2 generally indicates an unexpected DN value, but one which is physically possible from the camera itself. An IDQI of 1 flags data where the overclock and active pixel averages are not correlated as expected; and a IDQI value of 2 indicates an active pixel is saturated. It is noted that L1A Cal-CCD IDQI processing does not define a 2x2, 1x4, or 4x4 pixel as saturated by inspection of its neighbors or the red band 1x1 data value. The algorithms associated with these processes are described in §3.4.3.2.

### 3.3.3 Ancillary Radiometric Product data

#### 3.3.3.1 Out-of-range threshold parameters

These parameters are used to identify saturated data and anomalous conditions in which the science data quality may be compromised. The following parameters are included:

- (1)  $DN_{pix\_sat}$ , a data number threshold above which a pixel or sample of data is considered saturated. As the MISR instrument transmits 12-bit square-root encoded digital numbers ( $DN_{12}$ ), the maximum 14-bit numbers ( $DN_{14}$ ), after reversal of the encoding, would have a value of 16376. (The algorithm for reversing the square-rooting encoding is  $DN_{14} = \text{floor}((DN_{12}/32)^2 + 0.5)$ , and the maximum value of  $DN_{12}$  is 4095). Thus, any  $DN_{14}$  greater than or equal to 16376 is considered saturated.
- (2)  $n_{pix\_sat}$ , a threshold on the number of saturated pixels in a line. If the number of saturated pixels exceeds  $n_{pix\_sat}$ , the entire line is considered unusable.
- (3)  $DN_{line\_sat}$ , a data number threshold which, if exceeded by the average data number across a given line, indicates a potential reduction in accuracy of the radiance scaling process.

- (4)  $a_{pix\_sat}(0)$  and  $a_{pix\_sat}(1)$ , coefficients established from pre-flight testing and used to determine an estimate of the error in  $D_{overclock}$  which results from pixels in the array exceeding  $DN_{pix\_sat}$ .
- (5)  $\Delta DN_{line\_sat}$  a value established from pre-flight camera testing which gives the error in  $D_{overclock}$  which results from the average data number across a given line exceeding  $DN_{line\_sat}$ .

### 3.3.3.2 Detector Data Quality Indicators

The ARP provides Detector Data Quality Indicators (DDQIs) for each sample of data acquired by the MISR cameras. These values are related to the performance of the detector, and are updated as needed. Opportunities for revisions occur at the time of generation of a new version of the ARP (approximately monthly). These data quality indicators take on values indicating whether the data are within specifications on accuracy, signal-to-noise ratio, local uniformity, etc., or are otherwise of reduced quality. The latter condition may result, for example, from failure of a detector element, or a pinhole white-light leak in the filter above a particular pixel. These data quality indicators are not expected to change on rapid time scales.

The DDQIs take on the following values:

- DDQI = 0: Within specifications.
- DDQI = 1: Reduced accuracy.
- DDQI = 2: Available, but not usable for science.
- DDQI = 3: Unusable for any purpose.

The definitions of reduced accuracy and not usable for science are defined in a controlling document, see [IFRCC ATB, Section 4.10]. Unusable for any purpose implies the data are not related in any way to the incident radiance fields; and within specification indicates that there are no known instrument or data processing anomalies that degrade the quality of the data.

### 3.3.3.3 Radiometric calibration coefficients

Radiometric calibration coefficients are required for transforming Level 1A digital numbers (DN) to radiances. The MISR calibration equation uses three such coefficients for each data sample, and a quadratic relationship is established between radiance and DN. The coefficients are provided for each averaging mode of the MISR instrument. However, we note that since the 1x4 mode averages data in the along-track direction only, the output from the same detector element is used in the averaging; this means that the coefficient for 1x1 (unaveraged) and 1x4 data are the same. Pre-flight testing has shown the calibration to be insensitive to temperature over the operating range of the instrument. Thus, it is not considered necessary to provide calibration coefficients at other than the nominal orbital temperature.

#### **3.3.3.4 PSF deconvolution functions**

These normalized functions are provided for each averaging mode of MISR data, and are used in the image restoration process to correct for low-level halos that were observed during pre-flight camera testing.

### **3.4 THEORETICAL DESCRIPTION**

The MISR radiometric requirements determine the need for, and complexity of, the various calibration activities. In addition, algorithms developed for DAAC processing must provide a measure of incident radiance to these specifications. These requirements are specified in [ISR], [FDR], and [DPS]. All specifications listed refer to a  $1\sigma$  confidence level. Note that these requirements are specified for spatially and spectrally uniform, lambertian, and unpolarized scenes. Additional requirements on point-spread function and modulation transfer function response, spectral out-of-band rejection, and polarization sensitivity have also been levied on the MISR instrument.

**Absolute radiometric response:** The absolute radiometric uncertainty of the calibrated radiances of each MISR camera shall be no greater than 3% at 100% equivalent reflectance and 6% at 5% equivalent reflectance.

**Relative pixel-to-pixel response:** The maximum pixel-to-pixel radiometric uncertainty shall be no greater than 0.5% at 100% equivalent reflectance and 1.0% at 5% equivalent reflectance.

**Relative band-to-band response:** The maximum band-to-band radiometric uncertainty shall be no greater than 1.0% at 100% equivalent reflectance and 2.0% at 5% equivalent reflectance.

**Relative camera-to-camera response:** The maximum camera-to-camera radiometric uncertainty shall be no greater than 1.0% at 100% equivalent reflectance and 2.0% at 5% equivalent reflectance.

The following sections provide the theoretical basis behind the various processing steps depicted in Figure 3.3.

#### **3.4.1 Reverse square-root encoding**

##### **3.4.1.1 Processing objectives**

As described in §3.3.1, MISR IDNs are compressed to 12 bits through square-root encoding. In this step, this is reversed, to provide a 14-bit output (the original quantization level of camera data). It is these Level 1A DN values which are used as input to the Level 1B1 processing.

### 3.4.1.2 Mathematical description of the algorithm

Within the instrument, conversion from 14-bit camera output to square-root encoded 12-bit values is accomplished through the use of a programmable chip containing a look-up table. We simply utilize this look-up table in reverse in the ground data processing software. If this reversal results in multiple 14-bit numbers being associated with a given 12-bit input, we take the 14-bit output to be the mean of the set of 14-bit integers, rounded off to the nearest integer.

## 3.4.2 Radiance scaling

### 3.4.2.1 Processing objectives

The generation of calibration coefficients from sensor calibrations and radiance conversion algorithms must be such that the radiometric requirements are met. The calibration equation used for sensor calibration is an approximation to the actual sensor radiometric transfer curve (relating sensor output to radiance input). It shall contain a sufficient number of terms such that the accuracy of calibration is not limited by this parameterization.

### 3.4.2.2 Mathematical description of the algorithm

The specific form of the calibration equation is chosen such that it represents the actual radiometric transfer curve at all radiance levels, and is based on pre-flight camera test data. Pre-flight camera testing has demonstrated that the inclusion of higher order terms beyond the conventional linear expression provides a more accurate representation.

The equation relating DN to incident radiance, used during radiometric calibration is:

$$D - D_{\text{overclock}} = G_0 + G_1 L^{\text{std}} + G_2 (L^{\text{std}})^2 \quad (3.1)$$

where  $D$  is data number,  $L^{\text{std}}$  is band-weighted radiance, assuming weighting by the standardized spectral response curves, and  $G_0$ ,  $G_1$  and  $G_2$  are the calibration coefficients. The coefficients  $G_0$ ,  $G_1$ , and  $G_2$  are applicable to each sample of camera data and are expected to be slowly varying over the course of the mission. Note that values of  $G_0$ ,  $G_1$  and  $G_2$  are provided in the ARP for each data averaging mode (the same set applies to 1x1 and 1x4).  $D_{\text{overclock}}$  is a term representing the contents of the CCD serial registers, determined by sampling the "overclock" portion of the CCD readout signal. It includes a baseline stabilization (BLS) signal that varies with a time constant of several line repeat times (~25), and is proportional to the average signal intensity over a single channel line array. Thus,  $D_{\text{overclock}}$  varies from line to line, and knowledge of its magnitude is necessary for each line of MISR data in order to correctly perform either radiometric calibration or radiance scaling.

In 1x1 and 1x4 averaging modes there are eight overclock samples transmitted with each line of science data. In 2x2 mode, there are four values provided with each line, and in 4x4 mode there are two values. The value of  $D_{\text{overclock}}$  that is referred to in Eqn. (3.1), and utilized in Eqn. (3.2) below, is the average of the set of values provided with each line of science data.

Radiance scaling involves inversion of Eqn. (3.1). When performing this during DAAC processing, the coefficients  $G_0$ ,  $G_1$ , and  $G_2$  are supplied by the ARP, and are applied on a sample by sample basis. The term  $D_{overclock}$  applies to every sample in a line equally, and is obtained from the readout of the CCD array for each line as described above. Thus, to obtain radiance from camera DN, we have

$$L^{std} = \frac{-G_1 + \sqrt{G_1^2 + 4(D - D_{overclock} - G_0)G_2}}{2G_2} \quad (3.2)$$

where we have chosen the positive root of the quadratic. Should the coefficient  $G_2$  be zero, implying a perfectly linear device, radiance is retrieved via the expression

$$L^{std} = \frac{D - D_{overclock} - G_0}{G_1} \quad (3.3)$$

The condition where  $G_1$  is zero represents a dead pixel. Such a condition can be checked for prior to implementation of Eqn. (3.3), as indicated by the DDQI flag for this pixel. Data from such a pixel should not be processed to produce a radiance, but rather identified as a condition where no radiance measurements are available.

### 3.4.3 Perform scene-dependent quality assessment

#### 3.4.3.1 Processing objectives

During acquisition of MISR data, several conditions can cause the data quality to be dynamically compromised. These are:

- (1) One or more data samples saturate, e.g., due to a surface glint. These data are unusable for Level 2 processing. Because of the manner in which the MISR cameras operate, as observed during pre-flight camera testing, saturated pixels affect the signal in neighboring detector elements within the CCD line arrays.
- (2) Situations in which the knowledge of the signal offset that is subtracted from each line during the radiance scaling step of Level 1B1 processing is reduced in accuracy. The data are considered usable, but of reduced quality. This can occur when the average signal across an entire line array exceeds a certain threshold. This condition was observed during pre-flight camera testing, and is described in [IFRCC Plan].
- (3) The term inside the square-root sign of Eqn. (3.2) is negative, resulting in the inability to perform radiance scaling.
- (4) A radiance calculated according to Eqn. (3.2) is negative.

The occurrences of conditions (1) - (4) are evaluated to establish a Scene-dependent Data Quality Indicator (SDQI) for each sample of radiance. The SDQI values take on the same significance as the IDQI definitions given in Table 1.1. For science data:

SDQI = 0: Within specifications.

SDQI = 1: Reduced accuracy.

SDQI = 2: Available, but not usable for science.

SDQI = 3: Unusable for any purpose.

The definitions of reduced accuracy and not usable for science are defined by the radiometric error parameters,  $\epsilon_{pix\_sat}(0)$ ,  $\epsilon_{pix\_sat}(1)$ ,  $\epsilon_{line\_sat}(0)$ , and  $\epsilon_{line\_sat}(1)$  as specified in the following two sections. Unusable for any purpose implies the data are not related in any way to the incident radiance fields; and within specification indicates that there are no known instrument or data processing anomalies that degrade the quality of the data.

For calibration data we have:

SDQI = 0: No known anomalies.

SDQI = 1: Overclock out-of-range.

SDQI = 2: Saturated pixels.

SDQI = 3: Data transmission errors.

### 3.4.3.2 Mathematical description of the algorithm: Part 1, L1A Cal-packets

#### *Notation*

Let the parameter SDQI(line,pixel) refers to a SDQI value of indices line and pixel. (The L1A Cal-CCD product will provide an IDQI 2-bit value every line and pixel.)

For a 1x1 camera configuration the number of pixels is 1520 for the array;

- DN(line,1:1504) are active pixels;
- DN(line,1505:1512) are shielded pixels;
- DN(line,1513:1520) are overclock pixels.

The number of pixels is reduced accordingly, depending on averaging mode. Often pixels are referred to as “samples” within the MISR team. For the purpose of this memo the terms pixel (a concatenation of “Picture + element”) is used synonymously with sample.

The notation SDQI(line,\*\_active), SDQI(line,\*\_sheild), and SDQI(line,\*\_over) denotes that the SDQI value is set to a specific constant for every active, shield, or overclock pixel, respectively. Of course the specific index values for each of these would vary, depending on averaging mode.

The notation  $SDQI(line, pixel\_active)$  or  $SDQI(line, pixel\_over)$  denotes that the SDQI value is computed based upon the DN value specific to that pixel. Thus, the algorithm must index over  $pixel\_active$  or  $pixel\_over$  DN values.

The notation  $time(line)$  refers to the time tag associated with the data packet. The parameter  $time(out-of-sync)$  refers to the time tag of a packet which is believed to be out-of-sync as identified as by its APID.

The indices  $c$ , for camera, and  $b$ , for band, are also used below. Other parameters are configuration parameters (i.e.,  $DN_{pix\_sat}(b)$ ) and are defined by their usage below.

The parameters  $DN_{pix\_sat}$ ,  $t_{start}$ ,  $DN_{min\_active}$ ,  $DN_{min\_over}$ ,  $DN_{max\_over}$ ,  $time\_window$ ,  $a0$ ,  $a1$ , and  $DN_{error}$  are used in the algorithms given below. They are to be placed in a configuration table, such that they can be changed without otherwise modifying the production code.

#### 3.4.3.2.1 *Shielded pixel*

- $SDQI(line, *_active)=0$
- $SDQI(line, *_shield)=3$
- $SDQI(line, *_over)=0$

##### *Description*

The active and overlock pixels are initialized as a SDQI of 0 (usable). The SDQI of the shielded pixels are set to 3 (unusable).

#### 3.4.3.2.2 *Data transmission errors*

- If  $time(line) \leq t_{start}$  sec of camera turn-on, then  $SDQI(line, *)=3$
- Let  $DN_{mean\_over} = \text{mean}[DN(line, pixel\_over)]$   
if  $DN(line, pixel\_active) \leq DN_{mean\_over}$  or  
if  $(DN(line, pixel\_active) \leq DN_{min\_active})$  then  $SDQI(line, *)=3$
- If  $DN(line, pixel\_over) \leq DN_{min\_over}$  then  $SDQI(line, *)=3$
- If  $DN(line, pixel\_over) \geq DN_{max\_over}$  then  $SDQI(line, *)=3$
- If  $|time(line) - time(out-of-sync)| > time\_window$  then  $SDQI(line, *)=3$

##### *Description*

These conditions are most likely to result from a data transmission error or an instrument out-of-sync condition. In this case the entire line is rejected by the in-flight processing code.

#### 3.4.3.2.3 Overclock and line average correlation

- If  $SDQI(line,*)=3$ , then the remaining steps can be omitted.
- For each line, let
$$DN_{mean\_over} = mean[DN(line, pixel\_over)]$$
$$DN_{mean\_active} = mean[DN(line, pixel\_active)]$$
$$DN_{estimate\_over} = a0(c,b) + a1(c,b) * DN_{mean\_active}$$

if  $DN_{mean\_over} \geq DN_{estimate\_over} + DN_{error}(c,b)$  then  $SDQI(line,*)=1$

if  $DN_{mean\_over} \leq DN_{estimate\_over} - DN_{error}(c,b)$  then  $SDQI(line,*)=1$

##### *Description*

The parameters  $a0$ ,  $a1$ , and  $DN_{error}$  are defined per camera,  $c$ , and band,  $b$ . If the active pixel average and over clock pixel average are not within some specified limits, then a flag is set for these data. Note, if a higher  $SDQI$  value is set, the higher value remains.

#### 3.4.3.2.4 Saturated active pixels

- If  $DN(line, pixel\_active) \geq DN_{pix\_sat}(b)$  then  $SDQI(line, pixel\_active)=2$

##### *Description*

Saturated pixels are physically possible, should the instrument degrade in performance or view a bright target. An example of the former might be to the creation of a filter pinhole. In the case where a pixel goes bad in this manner and reports a saturated  $DN$ , we would want to rewrite the in-flight calibration processing software to process lines of data for which specific pixels are allowed to have a  $SDQI$  value of 2. (This would be a future change to our approach, as currently we do not process data with an  $IDQI$  of 2 or 3).

#### 3.4.3.3 Mathematical description of the algorithm: Part 2, L1A Science-packets

When a given pixel in a CCD line array saturates, pre-flight camera testing shows that a region of pixels surrounding the saturated element are affected to the extent that the data may be considered, according to a conservative criterion on data quality, unusable. Pre-flight data show that this region is not centered on the saturated pixel. In addition, the video offset of pixels outside the unusable region is less accurately represented by  $D_{overclock}$ , due to the added offset associated with the saturation. This is of particular consequence at low signal levels. Based on these measurements, the above algorithm is implemented for all channels of data at 1x1 and 1x4 sampling for which Level 1A data indicate that the line contains one or more saturated pixels:

#### 3.4.3.3.1 Saturation of individual data samples

- (1) Identify all pixels for which  $DN \geq DN_{pix\_sat}$ , where  $DN_{pix\_sat}$  is the threshold value above which a DN is considered to be invalid. The parameter  $DN_{pix\_sat}$  is provided by the ARP. Set  $SDQI = 3$  for pixels with  $DN \geq DN_{pix\_sat}$ .
- (2) Let  $n_{sat}$  be the number of saturated pixels in the line. If  $n_{sat} \geq n_{pix\_sat}$ , set the  $SDQI = 2$  for the remaining pixels in the line, and skip the remaining steps.
- (3) If  $n_{sat} < n_{pix\_sat}$ , let  $n_i$  be the pixel number representing the position in the line array (a value in the range 1 to 1504) of the  $i^{th}$  saturated pixel.
- (4) Flag all pixels in the range  $n_i - n(0)$  to  $n_i + n(1)$ , where we set  $n(0) = 50$  pixels and  $n(1) = 137$  pixels and we ignore cases where  $n_i - n(0) < 1$  and  $n_i + n(1) > 1504$ . Using these values, the maximum width of the flagged region is  $n(1) - n(0) + 1 = 188$  pixels, or 1/8 the width of the array.
- (5) Because a saturated pixel may fall within the flagged region resulting from another saturated pixel, the regions may overlap. We now combine all contiguous flagged regions into a block. With an individual region width of 188 pixels, there are a minimum of 1 and a maximum of 7 large blocks. If the entire array is saturated, there would be only 1 block.

For lines in which the data were collected in 2x2 averaging mode, a similar procedure is followed. There are 752 samples in such a line of data. In this case, the following changes are made:

- (1) For averaged data, it is possible that an individual pixel was saturated but the average DN reported does not exceed the saturation threshold because the other data numbers incorporated in the average may be low. Nevertheless, the data are still to be considered corrupted. Thus, in addition to identifying all locations where  $DN > DN_{pix\_sat}$ , we also examine all pixels for which  $DN > DN_{pix\_sat}$  in the red band, which is nominally obtained with no pixel averaging. If a given pixel is saturated in the red band, the corresponding 2x2 samples (i.e., the samples containing the location of the unaveraged pixel) in all non-red bands are also considered saturated.
- (2) Let  $n_{sat}$  be twice the number of saturated samples in the line (the factor of 2 results from the averaging mode). If  $n_{sat} \geq n_{pix\_sat}$ , set the  $SDQI = 3$  for all samples that are considered saturated,  $SDQI = 2$  for the remaining samples in the line, and skip the remaining steps.
- (3) If  $n_{sat} < n_{pix\_sat}$ , then letting  $n_i$  be the location of the  $i^{th}$  saturated sample (a number in the range 1 to 752), flag all pixels in the range  $n_i - n(0)$  to  $n_i + n(1)$ , where  $n(0)$  and  $n(1)$  now take on the values 25 and 68, respectively, and we ignore cases where  $n_i - n(0) < 1$  and  $n_i + n(1) > 752$ . Thus, the flagged region maximum width is 94 samples, which is 1/8 the width of the array of 2x2 samples.

For lines in which the data were collected in 4x4 averaging mode, a similar procedure is followed. There are 376 samples in such a line of data. In this case, the following changes are made:

- (1) As with 2x2 data, if a given unaveraged pixel in the red band is saturated (i.e.,  $DN > DN_{pix\_sat}$ ), the corresponding 4x4 samples in all non-red bands are also considered saturated.
- (2) Let  $n_{sat}$  be four times number of saturated samples in the line. If  $n_{sat} \geq n_{pix\_sat}$ , set the SDQI = 3 for all samples that are considered saturated, SDQI = 2 for the remaining samples in the line, and skip the remaining steps.
- (3) If  $n_{sat} < n_{pix\_sat}$ , then letting  $n_i$  be the location of the  $i^{th}$  saturated sample (a number in the range 1 to 376), flag all pixels in the range  $n_i - n(0)$  to  $n_i + n(1)$ , where  $n(0)$  and  $n(1)$  now take on the values 12 and 34, respectively, and we ignore cases where  $n_i - n(0) < 1$  and  $n_i + n(1) > 376$ . Thus, the maximum region width is 47 samples, which is 1/8 the width of the array of 4x4 samples.

Once the blocks of saturated data are established, the following algorithm is used to set the SDQIs.

- (1) If the SDQIs were already established for the entire line due to there being an excessive number of saturated samples, skip the following steps.
- (2) For all samples within the blocks, set SDQI = 2.
- (3) Calculate the relative radiometric error in samples outside of the unusable blocks resulting from the uncertainty in  $D_{overclock}$ . Differentiating Eqn. (3.1) with respect to  $D_{overclock}$ , we obtain (dropping the superscript *std* on the radiances for simplicity):

$$\left| \frac{\Delta L}{L} \right| = \left| \frac{\Delta DN_{pix\_sat}}{G_1 L + 2G_2 L^2} \right| \quad (3.4)$$

(Should the denominator equal 0, set SDQI=2 and leave the radiance value unchanged).

where  $\Delta DN_{pix\_sat}$  is an estimate of the error in  $D_{overclock}$ , and is given by

$$\Delta DN_{pix\_sat} = a_{pix\_sat}(0) + a_{pix\_sat}(1) \cdot n_{sat} \quad (3.5)$$

- (4) If  $|\Delta L / L| > \epsilon_{pix\_sat}(0)$  for a given sample, SDQI = 1 for that sample. We set  $\epsilon_{pix\_sat}(0)$  to a nominal value of 0.5%.
- (5) If  $|\Delta L / L| > \epsilon_{pix\_sat}(1)$  for a given sample, SDQI = 2 for that sample. We set  $\epsilon_{pix\_sat}(1)$  to a nominal value of 10%.
- (6) For all remaining samples, SDQI = 0.

#### 3.4.3.3.2 Saturation of CCD serial registers due to large average DN across line

The value  $D_{\text{overclock}}$  is obtained for each line of data, and is utilized in Eqn. (3.2) in the calculation of radiances. During pre-flight testing, it was discovered that when the average value of data number across a given line is below a certain value, and there are no saturated individual pixels, the value of  $D_{\text{overclock}}$  contained in the first 8 overclock pixels provides an accurate representation of the value that is appropriate for the entire line. As the illumination level increases beyond this point, however, the overclock signal develops an uncertainty on the order of  $\Delta \text{DN}_{\text{line\_sat}}$ , which is approximately 20 DN. In this case the first 8 overclock pixels provide a reduced accuracy estimate of  $D_{\text{overclock}}$ . Thus, it is necessary to identify when this situation occurs.

The lines of data for which the accuracy of  $D_{\text{overclock}}$  is potentially reduced are when the average data number across a given line  $> \text{DN}_{\text{line\_sat}}$ . For these lines of data, we set the SDQI as follows. Calculate the relative radiometric error resulting from the uncertainty in  $D_{\text{overclock}}$ . It is given by

$$\left| \frac{\Delta L}{L} \right| = \left| \frac{\Delta \text{DN}_{\text{line\_sat}}}{G_1 L + 2G_2 L^2} \right| \quad (3.6)$$

(Should the denominator equal 0, set SDQI=2 and leave the radiance value unchanged). Now, if  $|\Delta L / L| > \epsilon_{\text{pix\_sat}}(0)$  for a given sample, SDQI for that sample is set to the larger of unity and the SDQI established in §3.4.3.3.1. If  $|\Delta L / L| > \epsilon_{\text{pix\_sat}}(1)$  for a given sample, SDQI for that sample is set to the larger of 2 and the SDQI established in §3.4.3.3.1. We set  $\epsilon_{\text{line\_sat}}(0)$  to a nominal value of 0.5% and  $\epsilon_{\text{line\_sat}}(1)$  to a nominal value of 10%.

#### 3.4.3.3.3 Mathematical failure of radiance scaling equation

It is required to establish whether the term  $G_1^2 + 4(D - D_{\text{overclock}} - G_0)G_2$  in Eqn. (3.2) is negative. If this occurs, Eqn. (3.2) does not have real roots, and it is not possible to calculate a radiance. For samples in which this occurs, SDQI = 3.

#### 3.4.3.3.4 Negative radiances

The MISR signal chains contain a “baseline stabilization” (BLS) circuitry which guards against video offset changes, in the event that the CCD dark level drifts. This could occur suddenly, for example, during spacecraft passage through an auroral storm. The BLS circuitry uses the overclock pixels from the most recent series of lines to determine a voltage level which is subtracted from the video signal. The time constant associated with the BLS voltage is on the order of 25 line repeat times. Inadvertently, the BLS video is proportional to the average scene illumination over this time response window. As a consequence, when there is a rapid transition from a high average signal across the array to a low average signal, the BLS may for a short time

be overestimated, driving certain data numbers to levels that correspond to negative radiances. Although this is expected to be rare, situations where Eqn. (3.2) returns a negative radiance need to be identified. For samples in which this occurs, we set  $SDQI = 3$ .

### **3.4.4 Establish combined data quality indicators**

#### **3.4.4.1 Processing objectives**

In this step, the DDQIs and SDQIs are combined together to provide an overall data quality assessment parameter, the Image Data Quality Indicator (IDQI). The IDQI represents the assessment of data quality that is input to Level 1B2 processing.

Because the Level 1B1 product is not routinely archived at the DAAC, the IDQIs will be bundled with the Level 1A product, which is archived. Thus, final writing of the Level 1A product to the storage medium is not performed until the IDQIs have been derived. Since the Level 1A DN are 14-bit numbers, these 14 bits will be put into the most significant bits (MSBs) of the 16-bit words which constitute the product. The 2 least significant bits (LSBs) will be used for storage of the IDQIs. This is an efficient way of storing the required information.

As discussed in §3.4.6, the Level 1A and Level 1B1 data will have a different format in that the Local Mode and Global Mode data are contained within a single data stream at 1A, but are separated into different outputs at 1B1. To maintain a complete Global Mode data set, the Local Mode imagery needs to be averaged to the appropriate Global Mode resolution and “spliced” into the swath image. Consequently, IDQIs must be generated for these averaged data as well. Therefore, IDQIs will also be provided with the Level 1B1 Global and Local Mode data as input to Level 1B2 processing. Level 1B2 resamples the MISR radiances to produce orthorectified terrain-projected and ellipsoid projected, co-registered images on a Space Oblique Mercator grid. Each of these projected radiances in the Level 1B2 Georectified Radiance Product (GRP) will also have a resampled Radiometric Data Quality Indicator (RDQI) associated with it. Generation of the RDQI involves resampling of the IDQIs (see [GRP ATB]).

#### **3.4.4.2 Mathematical description of the algorithm**

The IDQI is generated for each sample of radiance as follows:

$$IDQI = \max(DDQI, SDQI) \quad (3.7)$$

Note that a value of zero has been used to specify values of DDQI, SDQI, and consequently IDQI which correspond to data that are within specifications, and a value  $> 0$  indicates reduced quality or unusable data. This is because the case  $IDQI = 0$  is the most frequent occurrence, and corresponds to keeping the LSBs of the 16-bit Level 1A data as zeros, following placement of the 14-bit DN into the MSBs (effected simply by a multiplication by 4).

### 3.4.5 Radiance conditioning: Image restoration

#### 3.4.5.1 Processing objectives

During the testing of the engineering model cameras it was discovered that pinhole images produced point spread functions (PSF) with a central core and low-level wings that extend over a considerable number of pixels in the cross-track direction (i.e., along the array). The light extending beyond the illuminated pixel is called the halo and is the result of diffuse scattering of a portion of the incident light off the pixel. The light scattered by the pixel undergoes a second reflection at the glass/argon interface (125  $\mu\text{m}$  from the pixel) or the spectral filter (about 38  $\mu\text{m}$  from the pixel) and returns to the detector array. The spatial extent and intensity of the halo varies from array to array and camera to camera. Typically, the magnitude of the halo is  $10^{-3}$  of the central PSF peak, but because of its extended nature accounts for several percent of the energy within the PSF.

The radiometric error introduced by the presence of the halos increases with scene contrast. That is, a uniform scene will produce no errors while high contrast scenes can produce measurable radiometric errors. In particular, it has been shown that the first two flight cameras tested violated the “dark region in a bright field” contrasting target specification [ISR] when the camera PSF’s were modeled. Hence, the processing objective of the PSF response correction is to improve the image radiometric fidelity by deconvolving the PSF.

Camera test data show that the qualitative features of the PSF can vary depending on the location of the illuminating sub-pixel spot within a single pixel. However, the situation of a bright point source against a dark background is not very representative of real scenes. Therefore, a more reasonable PSF is generated by averaging over several intra-pixel locations. This procedure was tested on one line array and produced a nearly symmetric, field independent PSF. This averaged PSF is generated for each of the 36 line arrays and is stored in the ARP. From each of these PSF’s, a deconvolution function is generated and also stored in the ARP. These deconvolution functions are the input to the deconvolution algorithm described below.

The deconvolution functions were derived by Fourier transforming the PSF’s, taking the inverse of the resulting function, inverse Fourier transforming back to the spatial domain, and taking the real part of the result. Because the PSF’s are nearly symmetric, the imaginary parts of the deconvolution functions are negligible and reasonably ignored. Like the PSF’s, the deconvolution functions are normalized to unit area under the curve. This approach to deconvolution is often not attempted because the Fourier transform of the PSF in general may have zero crossings, in which case taking the inverse would result in singularities. Fortunately, each of the MISR camera PSF’s is well-behaved in the regard and this situation does not occur; the deconvolution functions are well-defined, therefore making this approach feasible. Additionally, image restorations often make use of the estimated noise power spectrum to effect a degree of smoothing in the result. For simplicity, that approach is not used here, and this is justified by the high signal-to-noise ratio of the MISR cameras. Finally, image restoration approaches often impose a condition of positivity on the restored image. Again for simplicity, and because the MISR PSF’s consist of a sharp central peak surrounded by a low-level halo, the algorithm does not make use of this condition, as retrieval of negative radiances is deemed

extremely unlikely. Nevertheless, a check is made for negative radiances and flag values are set for those samples where this condition may occur. A tally is made of frequency of occurrence of such events and recorded as quality assessment parameters.

The deconvolution process is basically an image-sharpening process. As a result, the magnitude of random noise in the restored image will be larger than in the unrestored data, even in images of relatively uniform targets. This will result in some loss of signal-to-noise ratio, but since the MISR cameras have such high SNR to begin with and the blur PSF's are to first order close to delta functions this is not deemed a significant problem. Nevertheless, this fact requires the deconvolution process to be applied to calibration imagery as well as Earth scene imagery, so that SNR evaluation during the IFRCC process, which makes use of images of the instrument's deployable Spectralon panels, will have undergone image restoration processing prior to SNR evaluation.

### 3.4.5.2 Mathematical description of the algorithm

The blurring of the ideal image by a space-invariant PSF can be stated mathematically as the following convolution integral

$$g(x) = \int a(x - x')f(x')dx' + e(x) \quad (3.8)$$

where  $f$  is the ideal image as a function of spatial location,  $x$ ,  $a$  is the PSF,  $e$  is the noise, and  $g$  is the degraded image. As described above, the noise term is ignored in the algorithm. In order to obtain the ideal image from the degraded or observed image, one needs knowledge of the deconvolution function which deblurs the PSF. Since these have been precalculated from the PSF's, they are obtained from the ARP during standard processing. The deconvolution algorithm then consists of a convolution of the deblur functions with the image data on a line by line basis.

Let the line of observed data,  $g$ , have  $N$  radiance samples (labeled 1 through  $N$ ) and let the full extent (non-zero values) of the PSF be  $2j + 1$  samples where it is assumed that the PSF is spatially invariant. Note that we use the term "samples" to refer to data values at either 1x1, 1x4, 2x2, or 4x4 averaging. Thus, in 1x1 mode, a sample is the same as a pixel. The ARP defines a deconvolution function for each of these averaging modes, though we observe that the functions for 1x1 and 1x4 modes are identical, because the pixel averaging is in the along-track direction whereas the deconvolution is cross-track.

The PSF transfers energy from outside the detector field of view into the active samples, thus, we must extend the observed and restored lines by  $j$  samples at each end. In addition, application of the deconvolution algorithm requires a continuous set of data across the observed image line, making it necessary to "fill in" radiance values in  $g$  which are not valid. An invalid radiance value is one for which IDQI = 3. All remaining samples are considered valid (that is, reduced quality data values, e.g., those for which IDQI = 1 or 2, as well as those for which IDQI = 0, are acceptable for use in this algorithm). The filling in of the array is done by assuming the

intensity of the edge samples continues outside the array, and by using linear interpolation between valid samples to bridge across invalid blocks. That is

$$g(x_k) = g(x_{k_1}) \text{ for } -j + 1 \leq k < k_1 \quad (3.9)$$

and

$$g(x_k) = g(x_{k_2}) \text{ for } k_2 < k \leq N + j \quad (3.10)$$

where  $k_1$  is the location of the first valid sample (nominally,  $k_1 = 1$ ), and  $k_2$  is the location of the last valid sample (nominally,  $k_2 = N$ ). Eqn. (3.9) and Eqn. (3.10) are also applied to the restored image  $f$ . For the input image  $g$ , we also linearly interpolate across invalid samples, i.e., if  $k_m$  is the location of a valid sample, and  $k_n$  is the next valid sample, where  $n > m + 1$ , then for any location  $i$ , where  $m < i < n$ , we “fill in” the line according to

$$g(x_i) = g(x_m) + \frac{(i - m)}{(n - m)} \cdot [g(x_n) - g(x_m)] \quad (3.11)$$

Note that this filling in is done only for the purpose of applying the deconvolution algorithm. Once a restored image  $f$  is generated, we set  $f(x_k) = g(x_k)$  for all sample locations  $k$  which had invalid data, and we also discard the extended samples that were added to  $f$  at either end of the line as required to implement the algorithm.

We now describe how the restored image  $f$  is generated from  $g$  [after applying Eqn. (3.9) - Eqn. (3.11)]. The following equation describes this process:

$$f(x_k) = \sum_{i=k-j}^{k+j} g(x_i) d(x_i - x_k) \quad k = 1, \dots, N \quad (3.12)$$

where  $d$  is the deconvolution function.

Note that the data for  $d$  obtained from the ARP must correspond to the particular averaging mode of the data.

After applying Eqn. (3.12), and setting  $f(x_k) = g(x_k)$  for all sample locations  $k$  which had invalid data, a final check of the restored image  $f(x_k)$  is made to insure that no negative values resulted from the deconvolution process. In the event that this occurs, the radiances in the affected samples are set to a fill value and the associated IDQIs are set to a value of 3.

### 3.4.6 Separate Global and Local Mode data

#### 3.4.6.1 Processing objectives

As discussed in §2.2, Local Mode provides high resolution images in all 4 bands of all 9 cameras for selected Earth targets, by inhibiting pixel averaging in all bands of each of the cameras in sequence. This process leads to high resolution imagery in all 36 instrument channels for targets measuring approximately 300 km in along-track length.

During this step of the processing, the Local Mode imagery is separated out from the rest of the data to create distinct, regional images. However, further processing is required in order not to leave a gap in the Global Mode swath data. Thus, the Local Mode images are also averaged to the appropriate resolutions for each channel, to simulate the camera configuration corresponding to the Global Mode data. These averaged results are then “spliced” into the Global Mode swath to provide a continuous pole-to-pole image. Note that this averaging is not performed until all other radiance scaling and conditioning processes have transpired, in order to take advantage of the additional information provided (e.g., detecting saturated pixels) by maintaining the high resolution as long as possible.

#### 3.4.6.2 Mathematical description of the algorithm

Averaging of 1x1 radiances to 1x4, 2x2, or 4x4 modes involves computing a straight, unweighted mean of the appropriate pixels. The IDQI associated with the resulting average is established as the maximum of the IDQI values associated with each of the pixels that were used in computing the mean.

### 3.4.7 Scale output

#### 3.4.7.1 Processing objectives

The results of the above processing consist of radiances existing in computer memory as floating-point numbers. Before creating temporary 1B1 data files that will be used as input to Level 1B2 processing, these numbers will be scaled to 14-bit integers. These are then padded to 16 bits, either by including the IDQIs in the least significant bits, or by putting zeros in the most significant bits and passing the IDQIs along to Level 1B2 as separate data.

#### 3.4.7.2 Mathematical description of the algorithm

The ARP will contain a band-maximum radiance,  $L_{\max}$ , that is to be used to scale and store the radiances computed as the output of Level 1B1 processing. These values of  $L_{\max}$  are used to scale the radiance as follows:

$$\text{Output} = \left\| 16376 \cdot \frac{L_{\text{std}}}{L_{\max}} \right\| \quad (3.13)$$

where Output is the integer representation of the computed radiance, and where the symbol  $\|$  denotes finding the nearest integer. Scaled radiances will range from 0 to 16376. Integer values 16377 through 16383 are reserved as flag values set in the Level 1B2 software. Either the radiance, or flag value (in the event of an unusable radiance value) are packed into the 14 most significant bits of a 16-bit field. The least two significant bits of the field are reserved for the Image Data Quality Indicator computed for the sample.

The manner of deriving the values of  $L_{max}$ , including methods of insuring that the output does not exceed the 14-bit range, is described in [IFRCC ATB]. Should a radiance value exceed the threshold value, the radiance will be set to an out-of-range fill value, and the IDQI for that pixel is set to 3.

### 3.5 PRACTICAL CONSIDERATIONS

#### 3.5.1 Numerical computation considerations

Processing load estimates for the Radiometric Product are provided in [DPSize].

#### 3.5.2 Programming and procedural considerations

Guidelines to be followed during algorithm development are described in [ADP].

#### 3.5.3 Configuration of software

One of the purposes of the ARP is to establish the numerical values of certain configurable parameters used within the software. This avoids “hard-wiring” specific values. The Radiometric Product will contain information indicating what version of the ARP file was used. The configurable parameters contained within the ARP are shown in Table 3.2. The values shown correspond to the at-launch settings. The column entitled “Section” indicates where in this ATB a description of the specific configuration parameter is found.

**Table 3.2. Contents of the ARP Configuration File**

Description	Value	Section
Number of 1x1 or 1x4 pixels to subtract from saturated pixel location to identify beginning of saturation block ( $n_{1x1}(0)$ )	50	§3.4.3.3.1
Number of 1x1 or 1x4 pixels to add to saturated pixel location to identify end of saturation block ( $n_{1x1}(1)$ )	137	§3.4.3.3.1
Number of 2x2 pixels to subtract from saturated pixel location to identify beginning of saturation block ( $n_{2x2}(0)$ )	25	§3.4.3.3.1

**Table 3.2. Contents of the ARP Configuration File (continued)**

Description	Value	Section
Number of 2x2 pixels to add to saturated pixel location to identify end of saturation block ( $n_{2 \times 2}(1)$ )	68	§3.4.3.3.1
Number of 4x4 pixels to subtract from saturated pixel location to identify beginning of saturation block ( $n_{4 \times 4}(0)$ )	12	§3.4.3.3.1
Number of 4x4 pixels to add to saturated pixel location to identify end of saturation block ( $n_{4 \times 4}(1)$ )	34	§3.4.3.3.1
Radiometric error threshold for setting SDQI = 1 ( $\epsilon_{pix\_sat}(0)$ )	0.5%	§3.4.3.3.1
Radiometric error threshold for setting SDQI = 2 ( $\epsilon_{pix\_sat}(1)$ )	010%	§3.4.3.3.1
Radiometric error threshold for setting SDQI = 1 ( $\epsilon_{line\_sat}(0)$ )	0.5%	§3.4.3.3.2
Radiometric error threshold for setting SDQI = 2 ( $\epsilon_{line\_sat}(1)$ )	10%	§3.4.3.3.2

### 3.5.4 Quality assessment and diagnostics

In addition to the IDQIs appended to the Level 1A product, ongoing instrument and calibration quality assessment is provided through the In-flight Radiometric Calibration and Characterization program, described in [IFRCC Plan]. Diagnostic measures such as the tracking of calibration coefficients with time, Fourier analysis to search for coherent noise, and SNR tracking to locate pixels of poor radiometric quality, are included in this process. Further information may be found in [IFRCC ATB]. Assessment of calibration integrity will be performed through the use of multiple calibration pathways and cross-comparisons with other instruments. The information resulting from this process is quasi-static, that is, updated on approximately monthly centers within the ARP.

Swath processing summaries will also be archived with the Level 1A product to provide statistics indicating how often anomalous data condition occurred, e.g., the frequency of saturated pixels, negative radiances, and the like.

### 3.5.5 Exception handling

Situations where missing data affect the application of a particular algorithm are identified throughout this document.

## 3.14 ALGORITHM VALIDATION

MISR makes use of multiple sources of calibration and characterization data. The pre-flight test and analyses plans, and OBC system are described in Chapter 2. Other sources of calibration data include vicarious calibration campaigns (the transfer calibration of MISR using other aircraft of in-situ measurements), and analysis of imaging data over heterogeneous targets. The scatter of data from a given calibration, and from one calibration type to another will be used

to determine the uncertainty in sensor calibration. Details of the plan are provided in [IFRCC Plan].

### **3.15 ALGORITHM DEVELOPMENT SCHEDULE**

A strategy for time-phased development of the algorithms for the products and datasets described in this document, and a listing of key development milestones, are provided in [IFRCC Plan].

## **4. ASSUMPTIONS AND LIMITATIONS**

### **4.1 ASSUMPTIONS**

The following assumptions are made with respect to the radiometric scaling and conditioning described in this document:

- (1) Unless demonstrated otherwise it is assumed that there are no consistent coherent frequencies in the imagery, and coherent noise filtering is therefore not required.
- (2) A quadratic relationship between incoming spectral radiance and camera output DN is assumed.

### **4.2 LIMITATIONS**

None identified.

## 5. REFERENCES

1. Meyer-Arendt, J.R. (1968). Radiometry and photometry: units and conversion factors. *Appl. Opt.* 7:2081-2084.